Effect of Charge Density on the Interaction between Cationic Peptides and Oppositely Charged Microgels

Helena Bysell,* Per Hansson, and Martin Malmsten

Department of Pharmacy, Uppsala University, P.O. Box 580, SE-751 23 Uppsala, Sweden

Received: February 24, 2010; Revised Manuscript Received: April 17, 2010

The effect of charge density on the interaction between cationic peptides and oppositely charged poly(acrylic acid-*co*-acrylamide) microgels was investigated together with effects of charge localization and interplay between electrostatic and hydrophobic interactions. The microgel charge content was controlled by varying acrylic acid/acrylamide ratios (25/75−100/0 mol %) in the microgel synthesis, whereas peptide charge density was controlled by using monodisperse peptides containing alanine and lysine in a series of repeated patterns (25−50 mol % lysine). Results show that peptide uptake in the microgels is largely determined by microgel charge density, whereas peptide-induced microgel deswelling kinetics is influenced by peptide charge density to a higher degree. Furthermore, electrolyte-induced peptide detachment is highly influenced by both microgel and peptide charge density. Thus, at high charge contrast, peptides could not be detached from the microgels, whereas reducing the charge density of either peptide or microgel promoted electrolyte-induced peptide release. The localization of charges in the peptide sequence also plays a significant role as the interaction strength increased for peptides where all charged groups are located at the end of the sequence, as opposed to homogenously distributed throughout the peptide. Such an asymmetrically charged peptide thus displayed higher uptake, faster deswelling response, and lower release degrees than its homogeneously charged analogue in microgels with high charge content, while these differences were absent for lower microgel charge densities. Hydrophobic substitutions (alanine → leucine) in the peptide chain at fixed charge content increased peptide binding strength and eliminated peptide detachment at high ionic strength. Theoretical modeling of the effect of peptide and microgel charge density on peptide-induced microgel deswelling gave good agreement with experimental results.

1. Introduction

Lightly cross-linked polyelectrolyte microgels are materials with properties interesting for a range of applications. For instance, the volume of these particles can be drastically changed upon changes in pH, ionic strength, temperature, and external magnetic fields or in the concentration of specific ions and metabolites.[1−4] In addition, ionic microgel can bind substantial amounts of oppositely charged substances, such as peptides and proteins, and release them upon changes in the external environment. Consequently, microgels have potential in catalysis,[5,6] photonics,[7,8] biomaterials,[9,10] and as protective and stimuli-sensitive carriers for protein and peptide drugs.[4,11−16] Although the details of the interactions occurring in oppositely charged microgel−protein/peptide systems remain to be firmly established,[17−23] comparisons with more extensively studied systems, such as oppositely charged linear macromolecules,[24−27] as well as surfactant−polymer systems,[28−35] may provide some information. For instance, the strong association of oppositely charged macromolecules is driven largely by electrostatic interactions, typically yielding complex coacervates or precipitates at close to stoichiometric charge ratios. The strength of the electrostatic interactions normally increases with the charge densities of the interacting species, whereas at low charge densities, the contribution from nonelectrostatic (e.g., hydrophobic) interactions is more dominating. Oligomerization/aggregation may reinforce these effects, as observed for both surfactants and proteins binding to oppositely charged gels and macromolecules.[36−38] As a consequence, the uptake and release of substances to/from oppositely charged polyelectrolyte gels at high charge contrast is driven largely by electrostatic interactions, and parameters such as peptide charge, pH, and ionic strength play major roles. Similarly, interactions in microgel−peptide systems with high charge contrast have previously been shown to be very strong and dominated by electrostatics, resulting in irreversible peptide binding, network collapse, and arrested core−shell structures.[17−19] By reducing peptide charge density, homogeneous peptide distributions are obtained and peptides can be successfully detached by increasing the electrolyte concentration.[20] However, for the controlled use of microgels as delivery systems for protein and peptide drugs much remains to be done to clarify electrostatic and other interactions determining peptide incorporation to, distribution within, and release from microgels.

Given the above, the aim of the present investigation was to further elucidate the effect of electrostatics in oppositely charged microgel−peptide systems, addressing effects of charge density of both peptides and microgels, as well as of peptide charge localization and hydrophobicity, in one comprehensive study. For these purposes, poly(acrylic acid-*co*-acrylamide) microgels were synthesized, varying the acrylic acid content from 25 to 100 mol %, while peptide charge density was controlled by designing monodisperse peptides with 16 amino acid long sequences, containing alanine (A) and lysine (K), in various repetitions, with a total number of lysine groups, i.e., positive charges, increasing from 4 to 8 (Table 1). Peptide−microgel

* To whom correspondence should be addressed. E-mail: helena.bysell@farmaci.uu.se.

10.1021/jp1016664
Published on Web 05/11/2010

TABLE 1: Properties of the Peptides Studied

peptide name	peptide sequence	net charge	% charged residues	HI[a]	mol wt (g/mol)
AAAK4	AAAKAAAKAAAKAAAK	+4	25	0.385	1384
AAK5	AAKAAKAAKAAKAAKA	+5	31	0.019	1441
AK8	AKAKAKAKAKAKAKAK	+8	50	–1.05	1612
AA-K5	AAAAAAAAAAAKKKKK	+5	31	0.019	1441
LK8	LKLKLKLKLKLKLKLK	+8	50	–0.05	2062

[a] Peptide mean hydrophobic index as calculated from Kyte−Doolittle scale[46]

TABLE 2: Amount of Reactants Added in the Microgel Synthesis

microgel (AAc/AAm)	AAc (g)	2 M NaOH (g)	AAm (g)	0.8 mM BIS (g)
25/75	0.65	2.7	1.95	6.5[a]
50/50	1.3	5.4	1.3	6.5[a]
75/25	1.95	8.1	0.65	6.5[a]
100/0	2.6	11	0	6.5[a]

[a] Each monomer solution was diluted to 20 mL with purified water.

interactions were monitored with micromanipulator-assisted light microscopy for monitoring microgel deswelling and reswelling in response to peptide binding and release, confocal microscopy to evaluate peptide distribution within microgels, and solution depletion measurements to estimate peptide uptake in microgels. In addition, the effects of microgel and peptide charge density on peptide binding and resulting microgel deswelling were analyzed theoretically.

2. Experimental Methods

2.1. Materials. For microgel synthesis, *N*,*N*′-methylenebisacrylamide, *N*,*N*,*N*′,*N*′-tetramethylethylenediamine (TEMED), ammonium persulfate, acrylic acid (AAc), and acrylamide (AAm) were obtained from Sigma-Aldrich, (Steinheim, Germany), while sorbitan monostearate (Span 60) was obtained from Carl ROTH (Karlsruhe, Germany). The peptides (AK8, AAK5, AAAK4, AA-K5, and LK8; Table 1) were synthesized by Biopeptide Co. (San Diego, CA). The purity of the peptides was confirmed to be >95% by MALDI-TOF MS analysis (Voyager, Applied Biosystems). All other chemicals were of analytical grade. Purified Milli-Q water was used throughout. For pH control, 5 mM buffer solutions of sodium phosphate monobasic/sodium phosphate dibasic were used. Sodium chloride was added to obtain the appropriate ionic strength.

2.2. Preparation and Characterization of Microgels. ***2.2.1. Microgel Synthesis.*** Poly(acrylic acid-*co*-acrylamide) microgel particles were synthesized by inverse suspension polymerization. In brief, 0.09 g of Span 60 was dissolved in 50 mL of cyclohexane, and the resulting continuous phase was preheated to 45 °C and stirred at 1100 rpm under a nitrogen atmosphere. The charge content in the microgels was controlled by varying the amounts of acrylic acid/acrylamide in the monomer solutions (25/75, 50/50, 75/25, and 100/0 mol %). Acrylic acid (AAc) was partly neutralized (60%) by dropwise addition of NaOH (2 M), followed by addition of acrylamide (AAm) and *N*,*N*′-methylenebisacrylamide (BIS) (1.8 mol %), and finally diluted with purified water to 20 mL, as displayed in Table 2. A 2.75 mL amount of the monomer solution was mixed with 30 μL of TEMED (accelerator) and 100 μL of 0.18 M ammonium persulfate solution (initiator) and added to the preheated continuous phase. The polymerization was allowed to proceed at 45 °C for 15 min, whereafter temperature was raised to 65 °C under a nitrogen atmosphere to prevent quenching by oxygen. The reaction was stopped after 30−45 min by addition of 40 mL of methanol. Gel particles were then left to sediment overnight and then washed repeatedly with methanol and dried in a vacuum oven (Lab-line, Melrose Park, USA).

2.2.2. Microscopy. The volume response of single microgels upon pH cycling (pH 7 → 10 → 2 → 7) at salt concentrations of 5, 20, and 100 mM was investigated using micromanipulator-assisted microscopy as described below. It was found that microgel swelling/deswelling was totally reversible when changing pH and/or ionic strength and that reversibility persisted beyond one swelling/deswelling cycle (Figure S1, Supporting Information).

2.2.3. Potentiometric and Conductometric Titration. Dried microgel particles were redispersed in 20 mM NaCl solution (0.1 wt %) and HCl (1 M) added to obtain pH 2. The microgel suspension was then titrated with 0.1 M NaOH while monitoring pH using a Metrohm 654 pH meter and conductance using a Metrohm 660 Conductometer (Zofingen, Switzerland). From the titration curves obtained (Figure S2, Supporting Information), the charge content of microgels was determined. The charge content in the microgels was found to increase linearly ($R^2 = 0.965$) with the amount of acrylic acid monomer incorporated into the polymerization and cross-linking reaction (Figure S2, Supporting Information).

2.3. Uptake of Peptides in Microgels. Peptide uptake in microgels was measured using a solution depletion method, as previously described.[18,20] In brief, 125 μL of peptide solution (in the concentration range 25−700 μM at pH 7.4 and ionic strength 20 mM) was mixed with 25 μL of microgel suspension (0.1 w/w %) and allowed to equilibrate for at least 48 h. The microgel−peptide complexes thus formed were separated by centrifugation at 3000 rpm for 10 min. The amount of peptides remaining in solution was determined by bicinchonic acid assay,[39] performing absorbance measurements on a Saphire plate reader (Tecan, Männedorf, Switzerland) at $\lambda = 562$ nm, and compared to the peptide concentration in a solution without gels. From this the amount of microgel-bound peptides (mmol of peptide/g of microgel) at various equilibrium concentrations was determined.

2.4. Montoring Peptide-Induced Microgel Deswelling/Swelling with Microscopy. Changes in microgel volume upon peptide binding and release were monitored by micromanipulator-assisted light microscopy using an Olympus Bx-51 light microscope (Olympus, Tokyo, Japan) equipped with an ONM-1 manipulator (Narishige, Tokyo, Japan) and a DP 50 digital camera (Olympus, Tokyo, Japan). Viewfinder, Studio 3.0.1 (Pixera, San Jose, CA) and Olympus DP-soft (Olympus, Tokyo, Japan) were used as software. Micropipets (10−20 μm in diameter) were prepared with a PC-10 puller and a MF-9 forger (both Narishige, Tokyo, Japan). Gel particles were captured by micropipet suction using an IM-5A injector (Narishige, Tokyo, Japan), placed inside a 2 mm diameter flow pipet, and flushed with peptide solution using a Peristaltic pump P-1 (Pharmacia, Uppsala, Sweden) at a flow rate of 1.8 mL/min. This experimental setup allows the peptide concentration outside the microgel particle to be unaffected by peptide uptake in the gels. Captured gel particles were photographed every 30 s using Viewfinder software. The gel particle diameter was measured using Olympus DP-soft software and the deswelling ratios expressed as V/V_0, where V is the volume of a gel particle after exposure to peptide for a certain time and V_0 the volume of the gel particle before addition of peptide at pH 7.4 and 20 mM

ionic strength. The peptide-length-dependent volume response of single microgel particles (~70−80 μm in diameter at pH 7.4, I = 20 mM) after binding of peptides was studied at a concentration of 5 μM for each peptide at pH 7.4 and an ionic strength of 20 mM. To further investigate the binding strengths and electrolyte-induced release of peptides from microgels, peptide-loaded gel particles were flushed with pH 7.4 buffer solution of ionic strength 20 mM for 10 min, followed by buffer replacement to 150 mM for 20 min and then back to 20 mM ionic strength again to be able to compare the final gel volume, as this itself is influenced by the ionic strength. The hydrophobic peptide LK8 was not soluble at 20 mM ionic strength and therefore studied at 10 mM ionic strength. For comparison, AK8 was also analyzed at this condition.

2.5. Peptide Distribution in Microgels. Peptides AAK5 and AA-K5 were labeled with Alexa488 during the synthesis, giving peptides C(Alexa488)-AAKAAKAAKAAKAAKA and C(Alexa488)-AAAAAAAAAAAKKKKK, respectively. The peptide molecular weight was thereby increased from 1441 to 2242 g/mol, influencing also the charge density and hydrophobicity of the fluorescently labeled peptides. To evaluate the peptide distribution in microgels, a total of 5 μL of microgel suspension was equilibrated for at least 24 h with 100 μL of Alexa 488-labeled AAK5 and AA-K5. The distribution and intensity of fluorescently labeled peptides in microgels was monitored with a Confocal Leica DM IRE2 laser scanning microscope (CLSM; Leica Microsystems, Wetzlar, Germany) using a 63 × 1.2 water objective and software Leica TCS SL. Due to a high degree of swelling and small microgel size, no contrast matching, as previously found necessary for probing protein distributions in chromatography beads, is needed.[40] To investigate the extent of electrolyte-induced peptide detachment, microgel-bound peptides were washed with buffer of 20 and 150 mM ionic strength by repetitive centrifugation (5 min at 3000 rpm). The microgel−peptide complexes were then equilibrated for another 24 h, and the distribution and intensity were monitored by CLSM as described above. To evaluate the average fluorescence intensity in the microgels, ROI (region of interest) analysis was performed.

2.6. Theoretical Analysis. ***2.6.1. Equilibrium.*** The description is based on that by Flory and co-workers[41] but extended to include a polypeptide as a mobile ionic species. The gel is assumed to be in equilibrium with a (bulk) liquid containing all mobile electroneutral components. For a 1:1 electrolyte, the chemical potential is everywhere assumed to be

$$\mu_{1:1} = \mu^0_{1:1} + RT \ln C_+C_- \quad (1)$$

where $\mu^0_{1:1}$ is the standard contribution, R is the ideal gas constant, T is the absolute temperature, and C_+ and C_+ are the concentrations of positive and negative ions, respectively. For the polypeptide salt (polypeptide chain of positive charge Z plus its counterions) we write

$$\mu_{pep} = \mu^0_{pep} + \mu_{el} + RT \ln yC_{pep} + ZRT \ln C_- \quad (2)$$

where μ^0_{pep} is the standard contribution including the entropy associated with the flexibility of the peptide chain (assumed to be constant), μ_{el} is the electrostatic contribution due to the electric field surrounding polypeptide chains, C_{pep} is the concentration of polypeptide, and y is an activity coefficient. In the liquid y = 1, while in the microgel

$$y = \frac{C^{gel}_-}{C^{gel}_{Ac} + C^{gel}_-} \quad (3)$$

where $C^{gel}_{Ac}$and C^{gel}_- are the concentrations in the microgel of network acetate groups and negative mobile ions, respectively. Equation 3 describes a statistical distribution of polypeptide ions between two states in the microgel, one associated with the network charges and one with the simple anions, where only the latter fraction (y) is free to translate in the network. The chemical potential of water in the microgel is

$$\mu^{gel}_w = \mu^0_w + \mu^{mix}_w + \mu^{def}_w \quad (4)$$

where μ^0_w is the chemical potential of pure water, μ^{mix}_w is the contribution from the entropy of mixing, and μ^{def}_w is the contribution from elastic deformation of the network. Included in μ^{mix}_w is the Flory−Huggins entropy of mixing water and network chains and the ideal entropy of mixing with the other ions

$$\frac{\mu^{mix}_w}{RTv_w} = C_0(\ln(1 - \varphi) + \varphi) - (C^{gel}_+ + C^{gel}_- + yC^{gel}_{pep}) \quad (5)$$

where C_0 is the molar concentration of pure water and φ is the volume fraction of network. For μ^{def}_w we use the model based on the inverse Langevin function of the fractional extension of a chain

$$\frac{\mu^{def}_w}{RTv_w} = \frac{\varphi}{p\bar{v}}\left\{\left(\frac{\varphi_0}{\varphi}\right)^{2/3} - \frac{1}{2} + \frac{3}{5p}\left(\frac{\varphi_0}{\varphi}\right)^{4/3} + \frac{99}{175p^2}\left(\frac{\varphi_0}{\varphi}\right)^2 + \frac{513}{875p^3}\left(\frac{\varphi_0}{\varphi}\right)^{8/3} + ...\right\} \quad (6)$$

where p is the number of statistical segments in a polymer chain between cross-links in the network and $\bar{v}$ is the molar volume per statistical segment. The first two terms in eq 6 correspond to the Gaussian expression in the Flory−Rhener theory. In the liquid outside the microgel the concentration of polypeptide is very small in comparison with the concentration of simple electrolyte. The chemical potential of water is then given by

$$\mu^{liq}_w = \mu^0_w - 2v_wRTC_{salt} \quad (7)$$

where C_{salt} is the total concentration of 1:1 electrolytes in the liquid. The electroneutrality condition for the microgel can be written

$$C^{gel}_+ = C^{gel}_{Ac}(1 - \beta) + C^{gel}_- \quad (8)$$

where β is the polypeptide-to-network charge ratio in the microgel. C^{gel}_{Ac} is related to φ and the degree of dissociation of the acidic groups on the network α by $C^{gel}_{Ac} = \varphi\alpha/\bar{v}_{Ac}$, where $\bar{v}_{Ac}$ is the molar volume of network per acidic group. The relationship between α and pH is obtained by assuming that all monovalent cations, including the hydrogen ion, have the same affinity for the gel, so that

$$\frac{[H^+]_{gel}}{[H^+]_{liq}} = \frac{C_+^{gel}}{C_{salt}} \tag{9}$$

from which it follows that

$$pH = pK_a + \log\left(\frac{\alpha}{1-\alpha}\right) + \log\left(\frac{C_+^{gel}}{C_{salt}}\right) \tag{10}$$

where K_a is the acid constant of the acidic groups in the microgel, set to 4.7 in all calculations.

The concentration of simple ions in the gel is obtained from eqs 1 and 8 and the condition $\mu_{1:1}^{liq} = \mu_{1:1}^{gel}$(Donnan equilibrium)

$$C_\pm^{gel} = \sqrt{\left(\frac{\alpha\varphi(1-\beta)}{2\bar{v}_{Ac}}\right)^2 + C_{salt}^2} \pm \frac{\alpha\varphi(1-\beta)}{2\bar{v}_{Ac}} \tag{11}$$

where the minus sign applies to $C_=^{gel}$. Swelling equilibrium is calculated from eqs 4−7 and the condition $\mu_w^{liq} = \mu_w^{gel}$ by first substituting for $C_\pm^{gel}$ and C_{pep}^{gel} in eq 5 using eq 11 and $C_{pep}^{gel} = \alpha\varphi\beta/\bar{v}_{Ac}$. For a polypeptide-free solution ($\beta = 0$) this allows α and by eq 10 also pH to be expressed as a function of φ. For a polypeptide solution at high pH ($\alpha = 1$) a relationship between β and φ is obtained which can be solved iteratively. This, in turn, is used to calculate the equilibrium concentration of polypeptide in the liquid. From the condition $\mu_{pep}^{liq} = \mu_{pep}^{gel}$ one obtains

$$\ln C_{pep}^{liq} = \frac{\Delta\mu_{el}}{RT} + \ln yC_{pep}^{gel} + Z\ln\frac{C_-^{gel}}{C_{salt}} \tag{12}$$

$\Delta\mu_{el} = \mu_{el}^{gel} - \mu_{el}^{liq}$ is calculated using the cylindrical Poisson−Boltzmann theory (PB). The polypeptide chain is modeled as a uniformly charged cylinder of radius 6 Å with a surface charge density of 264, 396, and 528 Å^3 for AK8, AAK5, and AAAK4, respectively, determined from the chemical structure of the polypeptide and the fraction of charged peptides in the chain using an average peptide group length of 3.5 Å.[18,42] In the liquid the polypeptide concentration is so low that the cell model is unnecessary. The same holds also as a good approximation for the gels where the free polypeptide chain is considered to be screened by simple salt and the fraction of polyelectrolyte not in complexes with polypeptide, the latter treated as a simple electrolyte. Hence, the total concentration of electrolyte is $C_{PB}^{gel} = C_=^{gel} + C_{Ac}^{gel} - \beta C_{Ac}^{gel}(1-y)$. PB calculations give, to a very good approximation, $\Delta\mu_{el}/RT = mZ\ln(C_{salt}/C_{PB}^{gel})$, with m equal to 0.35, 0.25, and 0.19 for AK8, AAK5, and AAAK4, respectively.

2.6.2. Kinetics. The rate of mass transfer from the bulk liquid to the gel surface at steady state is calculated from the peptide diffusion constant in water ($D_{liq} = 1.6 \times 10^{-10}$ m^2/s)[23] and the Sherwood number (Sh)[33,43]

$$\frac{dn}{dt} = 4\pi r(1 + Sh/2)D_{liq}(C_{bulk} - C_r) \tag{13}$$

$$Sh = 2.0 + 0.6(Re)^{1/2}(Sc)^{1/3} \tag{14}$$

$$Re = \frac{2v\rho r}{\eta} \tag{15}$$

$$Sc = \frac{\eta}{\rho D_{liq}} \tag{16}$$

where r is the gel radius, C_{bulk} and C_r are the polypeptide concentration in the bulk liquid and in the liquid at the microgel surface, respectively, v is the liquid flow rate, ρ is the liquid density, and η is the liquid viscosity. When the deswelling rate is controlled by polypeptide mass transfer to the gel surface ("stagnant layer control") the time to reach binding ratio β is

$$t = \frac{r_0^3}{3v_0 Z D_{liq}}\int_0^\beta \frac{1}{r(1 + Sh/2)(C_{bulk} - C_r)}d\beta \tag{17}$$

For weakly charged networks (25% AAc) eqs 1−12 and the relationship $r = r_0(\varphi_0/\varphi)^{1/3}$ provide the relationship between r, β, and C_r required to evaluate the integral in eq 17. For highly charged networks (100% AAc) displaying core/shell phase separation during polypeptide binding an empirical expression is used

$$V = f\beta V_\infty + V_0(1 - f\beta)^a \tag{18}$$

where f is the polymer-to-polypeptide charge ratio in the shell, V_∞ is the volume of the fully collapsed gel, and a is a parameter. The first term on the righthand side is the volume of the shell, and the second is the volume of the core. The parameter a is larger than 1 when the formation of the shell decreases the swelling ratio of the core network and smaller than 1 when the effect is the opposite; there is evidence of both cases in the literature.[23,31,33,34,44,45] Phase equilibrium in the gel implies constant C_r (see ref 44 for discussion). This simplifies the kinetics of core/shell gels. For the initial part of the binding process, where Sh can be approximated as constant and the contribution of the shell to the gel volume can be neglected, the use of eq 18 in eq 17 gives

$$\frac{V}{V_0} = (1 - kt)^{3a/(3-a)} \tag{19a}$$

$$k = Zv_0 D_{liq}(C_{bulk} - C_r)(1 + Sh/2)f(3 - a)/r_0^2 \tag{19b}$$

It follows that the initial slope is equal to $-3ka/(3 - a)$ and thus proportional to Z for polypeptides displaying the same relationship between V/V_0 and β.

3. Results and Discussion

3.1. Effect of Charge Density. Electrostatic attraction is likely to be a major driving force for peptide inclusion in oppositely charged microgels as binding of peptides is associated with the release of a large number of counterions. The charge density of both the peptide and the microgel network is therefore likely a major parameter controlling interactions in oppositely charged peptide−microgel systems. To investigate the effect

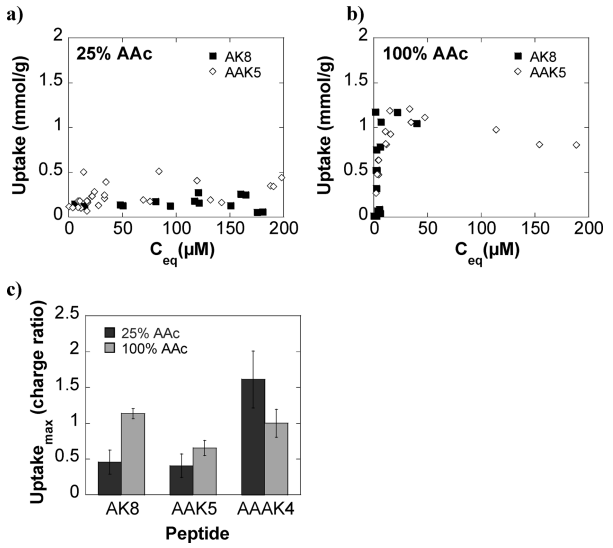

Figure 1. Influence of charge density on the uptake of peptides in microgels (mmol/g) as a function of equilibrium peptide concentration for AK8 and AAK5 binding to microgels containing 25% (a) and 100% (b) acrylic acid residues at pH 7.4 and ionic strength 20 mM. (c) Maximum uptake (molar charge ratio) for AK8, AAK5, and AAAK4 in microgels containing 25% and 100% acrylic acid residues.

of charge density on peptide uptake in poly(acrylic acid−acylamide) microgels, binding isotherms were obtained from solution depletion measurements. As can be seen in Figure 1, the equilibrium molar uptake of peptides was significantly higher for microgels containing 100% AAc than for lower charge microgels containing 25% AAc, and a substantially higher binding affinity was observed for the more highly charged microgel. Both effects are expected as microgels with a high charge content have a higher uptake capacity of oppositely charged substances. On the other hand, peptide charge density did not influence the peptide equilibrium uptake to the same degree as the uptake did not change significantly when going from 50% to 31% charged residues in the peptide chain (1.1 and 1.0 mol/g for AK8 and AAK5 in 100% AAc microgels) regardless of microgel charge. Taking into account the difference in the charge content of these peptides, these values correspond to limiting peptide/microgel charge ratios of 1.1 and 0.7 for AK8 and AAK5, respectively, indicating tighter complex formation for the more highly charged AK8. Strikingly, the highest peptide uptake was observed for the least charged peptide AAAK4 (containing only 25% charged residues) in both microgels containing 25% and 100% AAc residues (1.3 and 1.9 mol/g, respectively, corresponding to peptide/microgel charge ratios of 1.6 and 1). This high uptake, especially in microgels containing 25% AAc, emphasizes an increased influence of hydrophobic interactions for this modestly charged peptide. Although the hydrophobic/hydrophilic scaling of amino acid residues is complex and strongly varying between different scaling methods, AAAK4 is significantly more hydrophobic (0.38 on the Kyte and Doolittle scale) than AAK5 and AK8 (0.019 and −1.1),[46] increasing the probability for peptide self-association due to solubility limitations and possibly also nonelectrostatic interactions with hydrophobic domains in the microgel network.

To further elucidate the effect of charge density on peptide−microgel interactions, peptide-induced microgel deswelling was monitored with micromanipulator-assisted light microscopy. The peptide-induced deswelling response was found to increase with the peptide charge (Figure 2). Thus, final

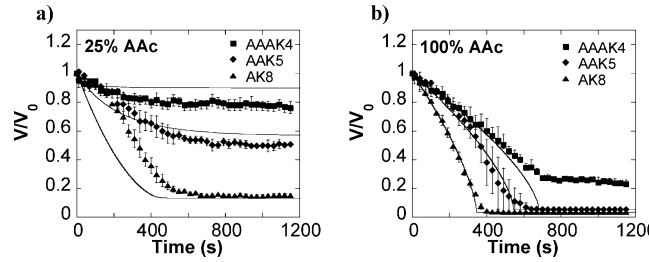

Figure 2. Effect of peptide charge density on microgel deswelling kinetics after addition of 5 μM peptide to microgels containing 25% (a) and 100% (b) acrylic acid residues at pH 7.4 and 20 mM ionic strength. The solid lines represent theoretical deswelling curves.

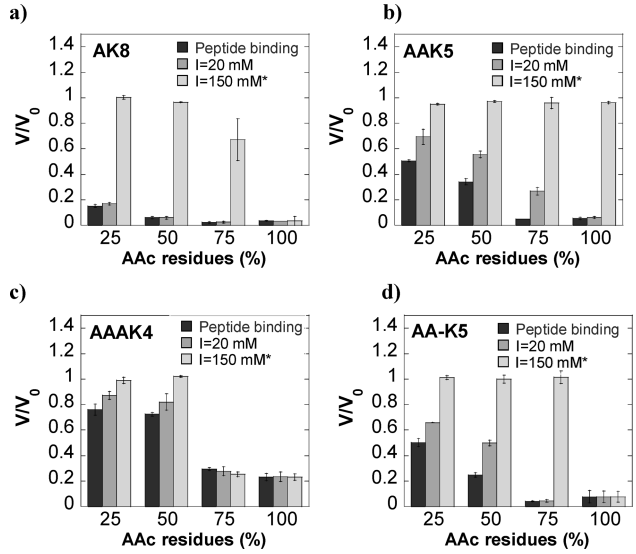

Figure 3. Volume ratio, V/V_0, of microgels of various charge content after exposure to 5 μM peptide solution (black) followed by a buffer solution of 20 mM ionic strength (dark gray) and a buffer solution of 150 mM ionic strength (light gray) at pH 7.4 for peptides AK8 (a), AAK5 (b), AAAK4 (c), and AA-K5 (d).

deswelling ratios (V/V_0) of 0.8, 0.5, and 0.15 were obtained for AAAK4, AAK5, and AK8 containing 25, 31, and 50 mol % charged amino acid residues, respectively, in the case of 25% acrylic acid microgels. The corresponding deswelling ratios for microgels composed of 100% acrylic acid were 0.2, 0.05, and 0.03, respectively. An analogous dependence of peptide charge was observed for microgels with 50% and 75% acrylic acid residues (Figure 3). These results are expected as the ion exchange from a peptide of higher charge density will be larger, thus inducing a larger osmotic contraction of the gel network. As will be discussed further below, results from theoretical modeling suggest that the presently investigated polypeptides are transported to, and taken up by, the microgels at similar rates. Furthermore, the microgel deswelling response is the same per peptide charge taken up regardless of peptide charge density, whereas the deswelling kinetics increases with increasing peptide charge since the number of charges carried by each chain increases. This is valid for microgels of lower charge degree, whereas the mechanism of peptide binding to highly charged gels is complicated by the formation of core/shell structures during incorporation.

The peptide−microgel interaction strength was further investigated by monitoring effects of peptide detachment after buffer equilibration at 20 mM ionic strength (same condition as the binding took place in) and subsequently increasing the ionic strength to 150 mM. When increasing the ionic strength, electrostatic interactions are screened and peptides bound to

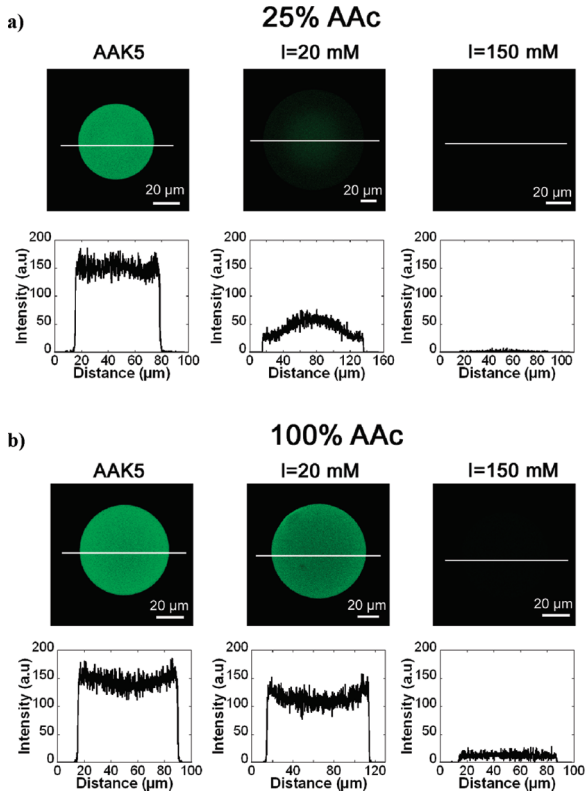

Figure 4. CLSM images and corresponding intensity profiles displaying the distribution of Alexa488-AAK5 in microgels containing 25% (a) and 100% (b) AAc residues after peptide binding and after washing with ionic strength 20 and 150 mM.

microgels at low ionic strengths are partially or fully detached from the network and released into the solution. Previous studies have shown peptide release to be influenced by peptide length.[20] Results obtained in the present study show that peptide release is dependent also on the charge density of both microgels and peptides. As shown in Figure 3, the peptide with the highest charge degree (AK8; 50 mol %, Figure 3a) displayed the highest interaction strength with microgels containing 100% AAc residues, as this peptide could not be detached from the highly charged gel network even when increasing the ionic strength to 150 mM. However, by reducing the AAc content (and charge density) in microgels to 75%, a partial release ($V/V_0 \approx 0.6$) of this peptide could be induced by increasing ionic strength. A further decrease in microgel charge content to 50% and 25% AAc residues yielded a complete release of AK8 ($V/V_0 = 1$) at 150 mM NaCl. For all microgel charge densities, interactions at 20 mM ionic strength were sufficiently strong to prevent peptide detachment during equilibration with low ionic strength, in accordance with previous results obtained for comparable systems.[20] The lower charge density AAK5 peptide (31 mol % charge, Figure 3b) was partially detached from all microgels, except those containing 100% AAc, already at 20 mM ionic strength and completely released from microgels regardless of microgel charge degree upon increasing the ionic strength to 150 mM. These results were also confirmed by peptide distribution measurements after peptide binding and after electrolyte-induced release, as displayed in Figure 4. Again, somewhat unexpectedly, the peptide of lowest charge degree (AAAK4; 25 mol %) bound very tightly to microgels of 75% and 100% AAc residues and could not be released by increasing ionic strength to 150 mM. However, this is in accordance with the high peptide binding observed for this peptide as discussed above and is probably due to increased hydrophobic or solvency-related interactions. A difference in appearance of microgels bound with AAAK4, compared to the more highly charged peptides, is also visible from microscopy images in Figure 5. Thus, granular features and a dense surface shell are observed for AAAK4, suggesting peptide aggregation/precipitation of AAAK4 in the highly charged microgels. As demonstrated before,[17,18] such dense shells are able to prevent uniform microgel deswelling, thus causing microgel deformation. In comparison, no such shell formation was observed for the higher charged AAK5 and AK8 peptides (Figure 5).

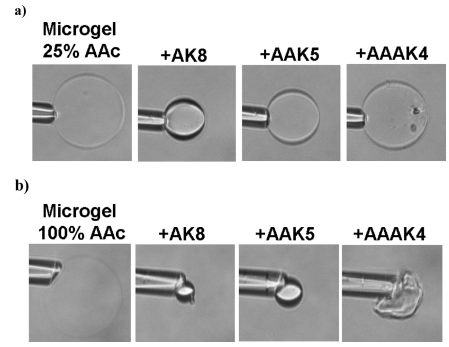

Figure 5. Exemplifying microscopy images showing microgels containing 25% (a) and 100% (b) acrylic acid residues before and after binding of AK8, AAK5, and AAAK4 (5 μM) at pH 7.4 and 20 mM ionic strength.

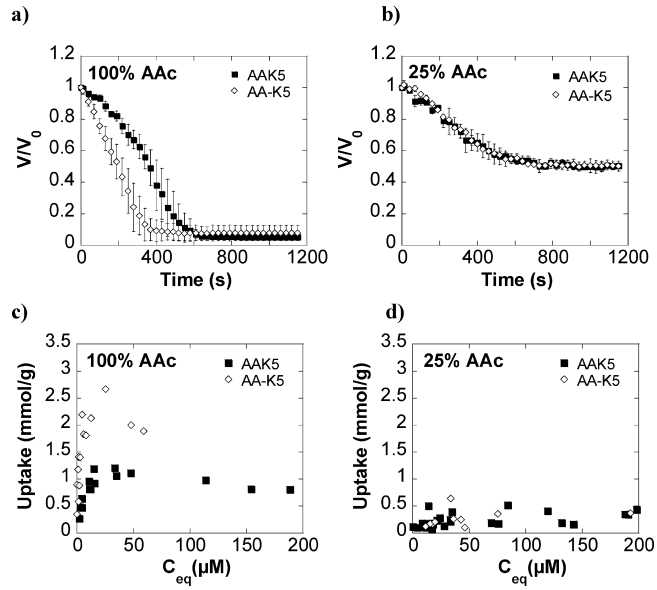

Figure 6. (a and b) Effect of peptide charge localization on microgel deswelling after addition of 5 μM peptides to microgels containing 100% (a) and 25% (b) acrylic acid residues. Shown also is the influence of charge localization on the uptake of peptides in microgels (mmol/g) as a function of equilibrium concentration for AAK5 and AAK-5 binding to microgels containing 25% (c) and 100% (d) acrylic acid residues at pH 7.4 and ionic strength 20 mM.

3.2. Effect of Charge Localization. The effect of peptide charge localization on peptide−microgel interactions was investigated by comparing the peptide AAK5, with 31% charged groups distributed homogenously over the peptide sequence, with the peptide AA-K5, with the same length and composition but all charges located at the end of the peptide sequence (Table 1). Figure 6a shows that at high charge contrast (i.e., for the gels containing 100% AAc residues) the peptide−microgel interaction strength is significantly increased when all charged peptide groups are located next to each other. This is reflected by a higher peptide-induced microgel deswelling response for

the AA-K5 peptide, as well as by a markedly reduced electrolyte-induced peptide release (Figure 3b and 3d). When lowering the charge content of the microgels to 50%, this effect was reduced (Supporting Information, Figure S4) and finally eliminated for 25% AAc microgels (Figure 6b). In analogy, the molar uptake of the block-charged AA-K5 (1.9 mmol/g) was substantially higher than for the homogeneously charged AAK5 in 100% AAc microgels but comparable in microgels containing 25% AAc (Figure 6c and 6d). These values correspond to peptide−microgel charge ratios of 1.3 and 0.7, respectively, for AA-K5 and AAK5 for the 100% microgel. Thus, by locating all charges at the end of the sequence, the peptide behaves essentially as a peptide with higher overall charge degree (i.e., AK8), with comparable charge ratios in the complexes formed, thereby also displaying the same microgel deswelling kinetics and inability to detach at increased electrolyte concentration. As a heterogeneous charge distribution induces amphiphilicity of the peptide sequence, it is possible that the microgel binding is reinforced by peptide self-assembly, in accordance with what is observed for cationic surfactants binding to poly(acrylic acid) microgels.[33,34,45] However, it is also likely that the charges in the block-charged AA-K5 peptide behave essentially as a single pentavalent charge, as the distance between these charges (∼4 Å) is smaller than the Debye length at 150 mM ionic strength (∼8 Å), thus contributing to the low release degree observed. Unfortunately, the different interaction strength observed for AA-K5 and AAK5 could not be demonstrated for the corresponding fluorescently labeled peptides by CLSM measurements (Figure S5, Supporting Information). Since the fluorescent tag is fairly large compared to the peptide size and also contains anionic residues, the properties of these small peptides can be expected to be rather substantially affected by the fluorescent group and thereby not necessarily display the same results as those observed for the untagged peptides.

3.3. Effect of Hydrophobicity. The interplay between electrostatic and hydrophobic interactions was further investigated by studying the effect of increasing the peptide hydrophobicity through alanine (A) → leucine (L) substitution in the AK8 peptide sequence, thereby obtaining peptide LK8 (Table 1). As shown in Figure 7 and Figure S6, Supporting Information, this substitution decreased peptide-induced microgel deswelling kinetics, similar to the effects found for AAAK4 but also for short peptides end tagged with hydrophobic amino acid stretches.[23] It seems that when sufficient hydrophobic groups are present in the interacting species, the peptide−gel complex layer formed precludes peptide diffusion in the microgels. As expected, the hydrophobically modified peptides are strongly bound to the microgels and cannot be detached with increased salt (Figure 7 and Figure S6, Supporting Information), indicating that electrostatic interactions are no longer the major parameter controlling the interactions in this system.

3.4. Theoretical Modeling. ***3.4.1. Swelling in Polypeptide-Free Solution.*** Figures S1a and S1b, Supporting Information, show results from theoretical modeling where the microgel diameter is plotted as a function of ambient pH for microgels with 25% and 100% AAc, respectively. The swelling response relative to the plateau at low pH, chosen to match the experimental diameters, is in qualitative or semiquantitative agreement with experimental data. In the model the pH-induced swelling is directly related to the ionization of the polymer, leading to an increased amount of mobile ions in the network. Already at low degrees of ionization the latter gives the dominating contribution to the swelling pressure. The opposing pressure due to elastic deformation of the network is calculated

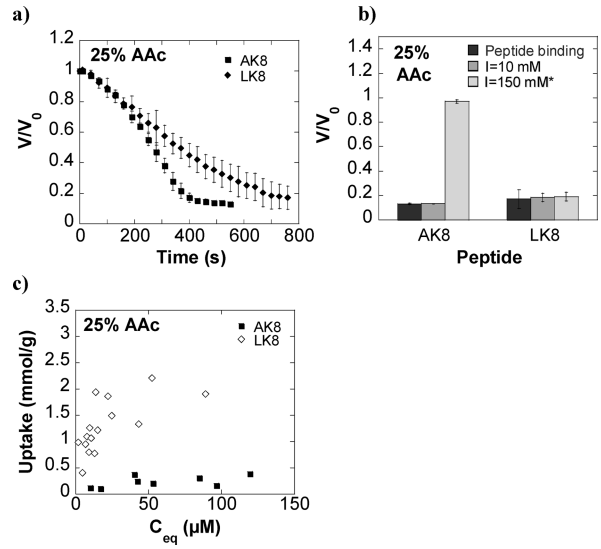

Figure 7. (a) Effect of peptide hydrophobicity on microgel deswelling after addition of 5 μM peptide to microgels containing 25% at pH 7.4 and 20 mM ionic strength. (b) Volume ratio, V/V_0, of microgels 5 μM peptide solution (black) followed by a buffer solution of 10 mM ionic strength (dark gray) and a buffer solution of 150 mM ionic strength (light gray) at pH 7.4. (c) Effect of hydrophobicity on peptide uptake in 25% AAc microgels at pH 7.4 and 10 mM ionic strength.

using the inverse Langevin expression, eq 6. However, nearly the same result is obtained with the Gaussian approximation. In agreement with the latter, the swelling approaches the scaling law $V/V_0 \approx \alpha^{6/5}$ at higher degrees of swelling. The fact that the exponent is close to 1 means that the volume increase is nearly proportional to the number of charges added to the network. The model takes into account neither counterion binding to the polyion nor the dependence of the flexibility of the chain on the degree of dissociation and the concentrations of salt and polyelectrolyte in the microgels, approximations reasonable for weakly charged polyions only. The agreement between theory and experiments in the 100% AAc case is therefore better than expected, possibly due to cancellation of errors. The swelling pressure should be overestimated since counterion binding is neglected. However, this may be compensated for by an overestimation of the opposing pressure from network elasticity, the latter calculated without considering that the stiffness of the chains should increase with increasing charge density and decreasing polyelectrolyte concentration.

3.4.2. Peptide-Induced Deswelling. The results from model calculations of the binding of AK8, AAK5, and AAAK4 to 25% AAc microgels in the presence of 20 mM salt are shown in Figures 2a and 8. For a given polypeptide-to-network charge ratio in the gel (β) the reduction of the microgel volume is independent of polypeptide charge density (Figure 8a). The reason for this is that the contribution from the peptides to the swelling pressure is so small in comparison to that from the small ions that the difference between them is masked. The peptides give a small contribution per charge since they are polymeric species and since they interact with the network chains. As a consequence, increasing β has nearly an identical effect on the gel volume as a decrease of α (see above). (It can be noted that the major part of the calculated relationship between gel volume and β is described well by the empirical law $V/V_0 = (1 - f\beta)^a$, with $f = 1$ and $a = 1$). In contrast, peptide charge density has a pronounced effect on the strength of binding to the microgels, as can be seen in Figure 8b, where β is shown as a function of the peptide concentration in the liquid in equilibrium with the microgel. The largest single contribution

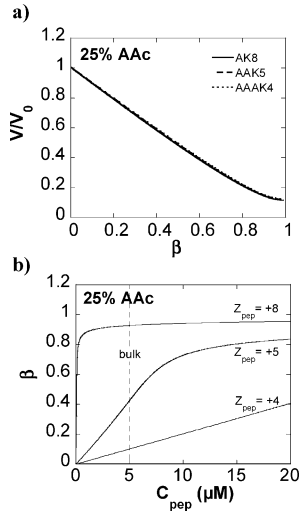

Figure 8. Results obtained from theoretical modeling describing the (a) deswelling ratios as a function of peptide-to-network charge ratio in the gel as well as (b) peptide-to-network charge ratio in the gels as a function of free peptide concentration for peptides of various charge densities interacting with microgels containing 25% acrylic acid residues.

to the effect comes from the gain in entropy per peptide chain from releasing network counterions, which increases with peptide charge (Z), as described by the last term in eq 12. There is also a contribution from the difference in the peptide electrostatic chemical potential as described by the first term in eq 12. While the former is a consequence of the Donnan equilibrium, the latter, which is smaller in magnitude, is directly related to the differences in linear charge density between the peptides. The kinetic peptide-induced microgel deswelling experiments are carried out at 5 μM bulk concentration of polypeptide. As evident from Figure 8a and 8b, the degree of binding at long times is expected to be substantially larger for the peptide with the highest charge than for the lower charged ones, therefore also corresponding to a larger decrease of the microgel volume. This can explain the differences between AK8, AAK5, and AAAK4 with respect to final gel volumes seen in the experiments (Figure 2a). In the same figure results from the kinetic model calculations are shown as solid lines. Evidently, the theoretically calculated final gel volumes are in good agreement with experiments. This is encouraging as there is no parameter fitting involved. The theory overestimates somewhat the initial decay rates, but the time to reach the final gel volume is in fairly good agreement with experiments. Importantly, the model captures the fact that the decay rate increases with peptide charge. It can be concluded that the different polypeptides are transported to and taken up at very similar rates to the microgel. The effect on the gel volume is the same per polypeptide charge taken up, but the deswelling rate increases with increasing peptide charge since the number of charges carried by each chain increases.

The lines in Figure 2b are the result of the kinetic modeling of the binding of the polypeptides to 100% AAc microgels. Also, in this case it is assumed that the deswelling rate is controlled by stagnant layer diffusion of the polypeptide. Equilibrium binding isotherms, calculated as for the 25% AAc case, indicate that a phase transition in the microgels takes place, consistent with the indications of core/shell phase coexistence during volume change in the experiments. However, quantitative calculations of core/shell transitions are complicated and lie outside the scope of the present paper. Instead, the curves in Figure 2b were calculated using eq 18 with $f = 1$ and $a = 0.55$ for all curves, the latter resulting from fit of the model to the experiments. The peptide concentration in local equilibrium with the gels (C_r) is expected to be negligible compared to the bulk concentration and is set to zero. Variation of a affects the shape of the calculated curves but has very small effects on the time to reach the fully collapsed state. This suggests that stagnant layer diffusion is the rate-controlling process also in this case, which can be explained by the low concentration in the bulk and the larger thickness of the stagnant layer compared with that of the shell. The observation that the model fits reasonably well during the first parts of all curves suggests that the peptides have a similar effect on the microgel volume per bound peptide charge and that the differences in decay rate are mainly attributed their charge numbers. The magnitude of a suggests an increased deformation ratio of the core network during shell formation. A possible scenario explaining this is that peptide transport though the shell is fast compared to the relaxation of the shell. Under such conditions peptides transported through the shell may quickly collapse layers of the core at the boundary to the core, giving rise to an outward pulling force on the core network chains.

4. Conclusions

Binding and release of cationic peptides to/from oppositely charged microgels is highly influenced by the charge density of both peptide and microgel. At high peptide−microgel charge contrast, stronger interactions are present, reflected in a high uptake of peptides in microgels, large peptide-induced microgel deswelling response, as well as limited peptide detachment from the microgel network at high ionic strength. Reducing the charge degree of microgel and/or peptide reduces the interaction strength, resulting in lower peptide binding, decreased peptide-induced microgel deswelling, as well as increasing peptide detachment from the microgels at high electrolyte concentrations. A heterogeneous distribution of positively charged groups in the peptide sequence, as well as hydrophobic modifications, also increases the interaction strength. Overall, results obtained in this study emphasize the importance of charge density, charge localization, and hydrophobicity in oppositely charged microgel−peptide systems and that those parameters can be controlled to tune the performance of microgels as stimuli-responsive carriers for protein and peptide drugs. Moreover, effects of microgel and peptide charge density on peptide-induced microgel deswelling can be well described and understood theoretically as being dominated by ion exchange.

Acknowledgment. This work was financed by the Swedish Foundation for Strategic Research and the Swedish Research Council. Martin Andersson is acknowledged for valuable discussions.

Supporting Information Available: Microgel volume in response to pH/salt cycling for microgels at various salt concentrations, conductometric/potentiometric titration curves and obtained microgel charge densities as a function of acrylic acid monomer, influence of peptide charge density on the deswelling kinetics of microgels with 50% and 75% AAc content, and effect of peptide charge localization as well as peptide hydrophobicity on 50% AAc microgels. This material is available free of charge via the Internet at http://pubs.acs.org.

References and Notes

(1) Dalmont, H.; Pinprayoon, O.; Saunders, B. R. *Langmuir* **2008**, *24*, 2834.

(2) Hoare, T.; Pelton, R. *Biomacromolecules* **2008**, *9*, 733.
(3) Saunders, B.; Vincent, B. *Adv. Colloid Interface Sci.* **1999**, *80*, 1.
(4) Thornton, P. D.; Mart, J. R.; Webb, S. J.; Ulijn, R. V. *Soft Matter* **2008**, *4*, 821.
(5) Lu, Y.; Mei, Y.; Ballauff, M.; Drechsler, M. *J. Phys. Chem. B* **2006**, *110*, 3930.
(6) Pich, A.; Karak, A.; Lu, Y.; Ghosh, A.; Adler, H.-J. *J Nanosci. Nanotechnol.* **2006**, *6*, 3763.
(7) Lyon, L. A.; Debord, J. D.; Debord, S. B.; Jones, C. D.; McGrath, J. G.; Serpe, M. J. *J. Phys. Chem. B* **2004**, *108*, 19099.
(8) Suzuki, D.; McGrath, J. G.; Kawaguchi, H.; Lyon, L. A. *J. Phys. Chem. C* **2007**, *111*, 5667.
(9) Jia, X.; Yeo, Y.; Clifton, R. J.; Jiao, T.; Kohane, D. S.; Kobler, J. B.; Zeitels, S. M.; Langer, R. *Biomacromolecules* **2006**, *7*, 3336.
(10) Saunders, B. R.; Laajam, N.; Daly, E.; Teow, S.; Hu, X.; Stepto, R. *Adv. Colloid Interface Sci.* **2009**, *147−148*, 251.
(11) Besheer, A.; Wood, K. M.; Peppas, N. A.; Mäder, K. *J. Controlled Release* **2006**, *111*, 73.
(12) Eichenbaum, G. M.; Kiser, P. F.; Dobrynin, A. V.; Simon, S. A.; Needham, D. *Macromolecules* **1999**, *32*, 4867.
(13) Li, Y.; de Vries, R.; Slaghek, T.; Timmermans, J.; Cohen Stuart, M. A.; Norde, W. *Biomacromolecules* **2009**, *10*, 1931.
(14) Morishita, M.; Goto, T.; Nakamura, K.; Lowman, A. M.; Takayama, K.; Peppas, N. A. *J. Controlled Release* **2006**, *110*, 587.
(15) Nolan, C. M.; Gelbaum, L. T.; Lyon, L. A. *Biomacromolecules* **2006**, *7*, 2918.
(16) Zhang, Y.; Zhu, W.; Wang, B.; Ding, J. *J. Controlled Release* **2005**, *105*, 260.
(17) Bysell, H.; Hansson, P.; Malmsten, M. *J. Colloid Interface Sci.* **2008**, *323*, 60.
(18) Bysell, H.; Malmsten, M. *Langmuir* **2006**, *22*, 5476.
(19) Bysell, H.; Malmsten, M. *Langmuir* **2009**, *25*, 522.
(20) Bysell, H.; Schmidtchen, A.; Malmsten, M. *Biomacromolecules* **2009**, *10*, 2162.
(21) Johansson, C.; Hansson, P.; Malmsten, M. *J. Colloid Interface Sci.* **2007**, *316*, 350.
(22) Johansson, C.; Hansson, P.; Malmsten, M. *J. Phys. Chem. B* **2009**, *113*, 6183.
(23) Bysell, H.; Hansson, P.; Schmidtchen, A.; Malmsten, M. *J. Phys. Chem. B* **2010**, *114*, 1307.
(24) Cooper, C. L.; Dubin, P. L.; Kayitmazer, A. B.; Turksen, S. *Curr. Opin. Colloid Interface Sci.* **2005**, *10*, 52.
(25) Dubin, P. L.; Bock, J.; Davies, R. M.; Schulz, D. N.; Thies, C. *Macromolecular Complexes in Chemistry and Biology*; Springer-Verlag: Berlin, Heidelberg, 1994.
(26) Kogej, K. Adv. Colloid Interface Sci. DOI: 10.1016/j.cis.2009.04.003.
(27) Wang, C.; Tam, K. C. *J. Phys. Chem. B* **2004**, *108*, 8976.
(28) Costa, D.; Hansson, P.; Schneider, S.; Graca, G.; Lindman, B. *Biomacromolecules* **2006**, *7*, 1090.
(29) Costa, D.; Miguel, M. G.; Lindman, B. *J. Phys. Chem. B* **2007**, *111*, 8444.
(30) Hansson, P. *Curr. Opin. Colloid Interface Sci.* **2006**, *11*, 351.
(31) Hansson, P.; Schneider, S.; Lindman, B. *J. Phys. Chem. B* **2002**, *106*, 9777.
(32) Kleinen, J.; Richtering, W. *Macromolecules* **2008**, *41*, 1785.
(33) Nilsson, P.; Hansson, P. *J. Phys. Chem. B* **2005**, *109*, 23843.
(34) Nilsson, P.; Hansson, P. *J. Phys. Chem. B* **2007**, *111*, 9770.
(35) Nilsson, P.; Unga, J.; Hansson, P. *J. Phys. Chem. B* **2007**, *111*, 10959.
(36) Karabanova, V. B.; Rogacheva, V. B.; Zezin, A. B.; Kabanov, V. A. *Polym. Sci.* **1995**, *37*, 1138.
(37) Zezin, A.; Rogacheva, V.; Skobeleva, V.; Kabanov, V. *Polym. Adv. Technol.* **2002**, *13*, 919.
(38) Carlsson, F.; Malmsten, M.; Linse, P. *J. Am. Chem. Soc.* **2003**, *125*, 3140.
(39) Smith, P. K.; Krohn, R. I.; Hermanson, G. T.; Mallia, A. K.; Gartner, F. H.; Provenzano, M. D.; Fujimoto, E. K.; Goeke, N. M.; Olson, B. J.; Klenk, D. C. *Anal. Biochem.* **1985**, *150*, 76.
(40) Malmsten, M.; Xing, K.; Ljunglöf, A. *J. Colloid Interface Sci.* **1999**, *220*, 436.
(41) Flory, P. J. *Principles of polymer chemistry*; Cornell University Press: Ithaca, NY, 1953.
(42) Nilsson, S.; Zhang, W. *Macromolecules* **1990**, *23*, 5234.
(43) Coulson, J. M.; Richardson, J. F.; Blackhurst, J. R.; Harker, J. H. *Coulson & Richardson's Chemical Engineering*; Butterworth-Heinemann: Oxford, 1996.
(44) Hansson, P. *J. Phys. Chem. B* **2009**, *113*, 12903.
(45) Nilsson, P.; Hansson, P. *J. Colloid Interface Sci.* **2008**, *325*, 316.
(46) Kyte, J.; Doolittle, R. F. *J. Mol. Biol.* **1982**, *157*, 105.

JP1016664